

Structural Study of Thermochromism in Poly(di-*n*-alkylgermanes) by Raman Spectroscopy in the Visible and Near-Infrared

V. M. Hallmark, C. G. Zimba, R. Sooriyakumaran, R. D. Miller, and J. F. Rabolt*

IBM Research Division, Almaden Research Center, 650 Harry Road,
San Jose, California 95120-6099. Received June 13, 1989;
Revised Manuscript Received October 13, 1989

ABSTRACT: UV-vis studies of symmetrically substituted poly(di-*n*-alkylgermanes) indicate that these polymers exhibit a thermochromic transition at temperatures considerably reduced from that of their polysilane counterparts. Fourier transform Raman spectroscopy using Nd:YAG excitation has been used in conjunction with thermal analysis and conventional Raman spectroscopy to assess the role of the side chains and the germanium backbone in the onset of thermochromism. In order to make a detailed band assignment, a series of Ge oligomers have been synthesized and investigated in both the melt and solid state. Their spectra were obtained using conventional Raman spectroscopy in the visible and the data used to differentiate between backbone and side-chain vibrations.

Introduction

Although many studies¹⁻⁶ of poly(di-*n*-alkylsilanes) in solution and the solid state have appeared in the literature, little has been written about their germanium-backbone analogues. The latter are also considered σ -conjugated systems and hence represent an interesting class of materials that absorb in the near-UV (330–370 nm), and as such were initially considered as potential candidates for lithography in this region. Interestingly enough, the symmetrically substituted poly(di-*n*-alkylgermanes), like their polysilane counterparts, exhibit order-disorder transitions; however, the temperature range of these transitions is considerably depressed relative to the silicon analogues. Whereas many of the poly(di-*n*-alkylsilanes) undergo a shift in UV-absorption maxima by as much as 60 nm at the onset of the transition temperature (42–74 °C), the alkyl-substituted polygermanes shift only 40–45 nm when their temperatures are lowered to that of the ordered state (–25 to +12 °C). Interestingly, the limiting absorption wavelength of poly(di-*n*-hexylgermane) below the transition temperature is the same as that observed for poly(di-*n*-hexylsilane) below 42 °C. Thus, although both the silicon and germanium polymers exhibit thermochromic behavior, the exact nature of this transition in poly(di-*n*-alkylgermanes) has yet to be investigated.

In general, little is known about order-disorder transitions since many characterization techniques require long-range order before structural information can be obtained. Vibrational spectroscopy, on the other hand, is unique because it can be used to assess the nature and amount of local order. In addition, the presence or absence of certain band splittings can be used to characterize the intermolecular environment of the polymer chain.

It is the purpose of this work to explore the structural changes that occur when the symmetrically substituted poly(di-*n*-alkylgermanes) are cooled to their ordered state. A new technique, FT-Raman spectroscopy,^{7,8} has been used in conjunction with thermal analysis and conventional Raman scattering to assess the role of order in the alkyl side chain in bringing about the transition. In addition, a mechanism for the reversible, thermochromic transition is proposed.

Experimental Section

A. Synthesis of Poly(di-*n*-alkylgermanes). Poly(di-*n*-hexylgermane). The monomer dichlorodi-*n*-hexylgermane and

the corresponding polymer (PDHGe) were prepared as described previously.⁹ The purified polymer sample used in this study had a M_w of 950 000 with a polydispersity of 1.7.

B. Preparation of 2,2-Di-*n*-butyl-1,1,3,3,3-hexamethyltrigermene. Into a dried flask were placed 0.492 g (0.07 mol) of Li (1% Na) powder and 25 mL of ether. A mixture of 6 mL (0.05 mol) of chlorotrimethylgermane and 3.0 g (0.01 mol) of dichlorodi-*n*-butylgermane in 25 mL of ether was added dropwise with stirring. The reaction was mildly exothermic. After the addition the reaction was stirred 2 h at 25 °C and refluxed for 1 h. The salts were filtered, and the sample was concentrated. The oil was diluted with pentane and refiltered. After removal of the pentane, the residue was distilled using a Kugelrohr (bp 55–105 °C (0.025 mm), 3.8 g). This material was chromatographed on alumina using hexane to yield 700 mg of the trigermene, which was >90% pure by GLPC analysis: IR (neat) 2960, 2923, 2873, 1461, 1406, 1376, 1230, 1170, 1081, 1002, 963, 814, 749, 687 cm⁻¹; ¹H NMR (CDCl₃) δ 1.31 (m, 8 H), (0.8–1.0, m, 10 H), 0.25 (s, 18 H); ¹³C NMR (CDCl₃) δ 30.1, 26.5, 13.6, 12.0, –0.3.

C. Preparation of Decamethyltetragermene. Into a dry flask were placed 0.4 g (0.057 mol) of lithium powder (1% Na) and 15 mL of ether. A solution of 6.5 g (0.043 mol) of chlorotrimethylgermane in 5 mL of ether was added dropwise at room temperature. After the addition, 20 mL of THF was added and an exothermic reaction occurred. The reaction was stirred for 1 h and filtered. After dilution with 100 mL of ether, the organic layer was washed three times with 50-mL portions of water and the organic layer dried over MgSO₄. The solvent was removed and the residue distilled (bp 109–112 °C) to yield 3.2 g of pure hexamethyldigermene, which was identical with a commercial sample purchased from ICN. A total of 3.0 g of hexamethyldigermene was slowly added to a suspension of 1.70 g of aluminum chloride and 1.0 g of acetyl chloride maintained at room temperature by external cooling. After 3 h of stirring the reaction mixture was extracted with pentane. The residue, after solvent removal, was purified by bulb-to-bulb distillation at 0.08 mm. The chloropentamethyldigermene produced in this manner was 94% pure by GLPC analysis: ¹H NMR (CDCl₃) δ 0.74 (s, 6 H), 0.38 (s, 9 H); ¹³C NMR (CDCl₃) δ 4.33, –2.66.

The product from above was dissolved in 10 mL of THF and stirred with 0.06 g (0.008 mol) of lithium powder (1% Na) for 6 h at room temperature. The mixture was diluted with pentane and filtered, and the solvent was removed. The decamethyltetragermene was purified by Kugelrohr distillation [100 °C (0.08 mm)] to yield 100 mg of product, which was >96% pure: ¹H NMR (CDCl₃) δ 0.47 (s, 12 H), 0.33 (s, 18 H); ¹³C NMR (CDCl₃) δ –1.19, –4.88; mass spectroscopic empirical formula Ge₄C₁₀H₃₀.

D. Conventional Raman Measurements. Visible excitation at 4880 Å was provided by a Spectra-Physics 2020 argon

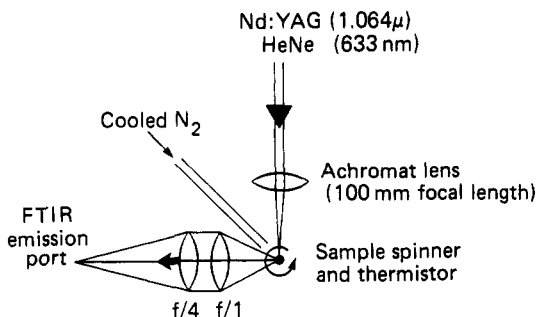


Figure 1. Schematic diagram of N_2 -cooled sample spinning arrangements used to obtain FT-Raman spectra at low temperature.

ion laser at incident powers of approximately 100 mW. Raman spectra from a 90° scattering geometry were recorded with a Jobin-Yvon HG2S double monochromator, fitted with a cooled, RCA 31034 photomultiplier tube, using standard photon-counting electronics. Data were collected and digitally processed by a Nicolet 1180 data system. Spectral resolution was typically 3 cm^{-1} .

E. FT-Raman Spectroscopy. A brief description of the FT-Raman system utilized for these measurements follows, but more detailed specifications are available elsewhere.^{7,8} Excitation at $1.064\text{ }\mu\text{m}$ was provided by a Spectron Laser Systems, Model SL50, CW Nd:YAG laser, coupled to an Applied Photophysics laser monochromator to remove the competing laser line at $\sim 1.3\text{ }\mu\text{m}$ and residual flashlamp emission. A He:Ne laser was introduced collinearly with the invisible Nd:YAG to ensure ease and safety during alignment procedures. A typical excitation power of 0.5 W focussed onto the sample by a standard, 100-mm-focal-length lens, induced sample degradation, but this problem was overcome by reducing power density via sample spinning (Figure 1). Cooling was accomplished by directing a stream of nitrogen gas after passage through a liquid-nitrogen heat exchanger onto the spinning-sample capillary. Temperatures were varied by gas flux and measured by mounting a thermistor adjacent to the sample position. Scattered light was collected at right angles by the $f/1$ side of an air-spaced double lens, which then focussed the light at $f/4$ onto the emission port of a Bomem DA3.02 Fourier transform interferometer. The interferometer was equipped with a quartz beam splitter and a thermoelectrically cooled (-35°C) indium-gallium-arsenide detector. Rayleigh scattering was rejected by a set of Microcoatings dielectric filters, allowing measurements down to 500 cm^{-1} . Spectral resolution in all cases was 4 cm^{-1} .

Results and Discussion

A. Vibrational Assignments. Since very little work⁹ has been done on polygermanes or their finite-chain oligomers, a representative dimer, trimer, and tetramer were investigated in order to assign bands to specific vibrations of the Ge-C and Ge-Ge bonds. Although the oligomers used in this study were not isostructural with the polymer, localized vibrations of Ge-C bonds should not be influenced significantly by the molecular structure. This is borne out by the spectra shown in Figure 2. In the region between 550 and 650 cm^{-1} , at least two bands located at 570 and 590 cm^{-1} can be assigned to stretching of the Ge- CH_3 bond. Likewise, in the trimer, which has two butyl groups attached to the central Ge, a third band can be identified at 633 cm^{-1} and attributed to a stretch of the Ge- CH_2 bond. It is this latter vibration that should also be observed in the symmetrically substituted poly(di-*n*-alkylgermanes).

In the region below 300 cm^{-1} , bands assignable to Ge-Ge stretching vibrations are expected. As shown in Figure 2, the low-frequency spectra of the oligomers become increasingly complex as the number of backbone atoms

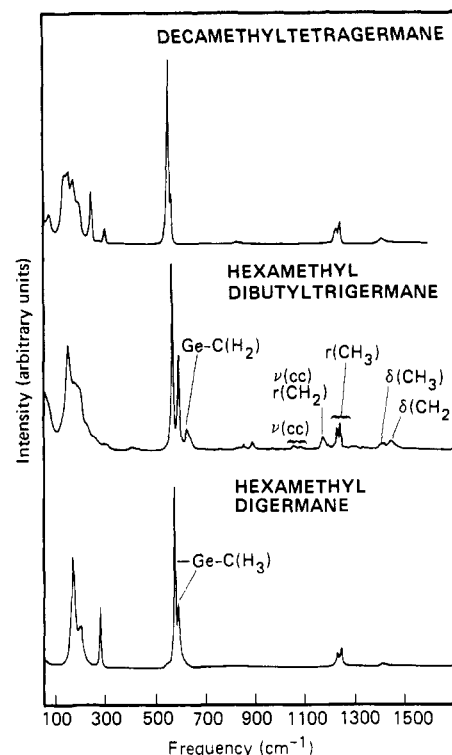


Figure 2. Raman spectra (50 – 1500 cm^{-1}) of low molecular weight germane oligomers obtained at room temperature in the liquid state.

increases. This must, in part, result from a mixing of the Ge-Ge stretches with torsional motion of the backbone, and it makes it nearly impossible to assign the wealth of bands observed in this region.

The final region where some insight into band assignments for the polymer can be obtained from oligomers is the 1000 – 1500 cm^{-1} region of the trimer where a weak to medium intensity band is found at 1174 cm^{-1} . It is not present in the spectrum of either the methyl-substituted dimer or tetramer and, hence, is associated with the butyl groups attached to the central Ge. In a previous study¹⁰ of asymmetrically substituted poly(di-*n*-alkylsilanes), a band was observed at 1182 cm^{-1} and assigned to stretching of the C-C bond immediately adjacent to the Si-C bond. This assignment was supported⁶ by investigation of a ^{13}C -enriched sample of PDHS where, after isotopic substitution of the α -carbon of the alkyl side chain, this band was observed to shift to 1176 cm^{-1} . In an analogous fashion, the 1174 cm^{-1} band found in the trimer is assigned to the C-C stretching vibration of the bond immediately connected to the Ge backbone. As will be discussed in a later section, it is this same band that has its intensity enhanced when Raman spectra are recorded using visible excitation.

A number of other bands in this region can be assigned by a comparison of the oligomeric spectra shown in Figure 2. A weak band found at 1412 cm^{-1} in all three oligomers can be confidently assigned to a scissoring motion ($\delta(\text{CH}_3)$) of the H-C-H groups of the methyl group. In a likewise fashion, the weak feature found at 1447 cm^{-1} only in the trimer spectrum can be attributed to a similar motion ($\delta(\text{CH}_2)$) of the CH_2 groups.

The medium doublet at $1232/1244\text{ cm}^{-1}$ is again observed in all three oligomers and is assignable to the rocking vibration ($r(\text{CH}_3)$) of the methyl groups. The corresponding $r(\text{CH}_2)$ band should be present in the spectrum of the trimer and its most likely location is coincident with the 1174 cm^{-1} CC stretching vibration discussed earlier. Snyder et al.¹¹ have shown that the

Table I
Observed Frequency (cm^{-1})

dimer	trimer	tetramer	assignment ^a
573	567	577	$\nu(\text{Ge-CH}_3)$
		584	
589	591	593	$\nu(\text{Ge-CH}_3)$
	633		$\nu(\text{Ge-CH}_2)$
	1053		$\nu(\text{C-C})$
	1063		$\nu(\text{C-C})$
	1083		$\nu(\text{C-C})$
	1174		$\nu(\text{CC}), \text{r}(\text{CH}_2)$
1231	1232	1229	} $\text{r}(\text{CH}_3)$
1246	1244	1239	
1410	1410	1412	$\delta(\text{CH}_3)$
	1423		} $\delta(\text{CH}_2)$
	1447		
	1459		

^a ν , stretch; r, rock; δ , scissors.

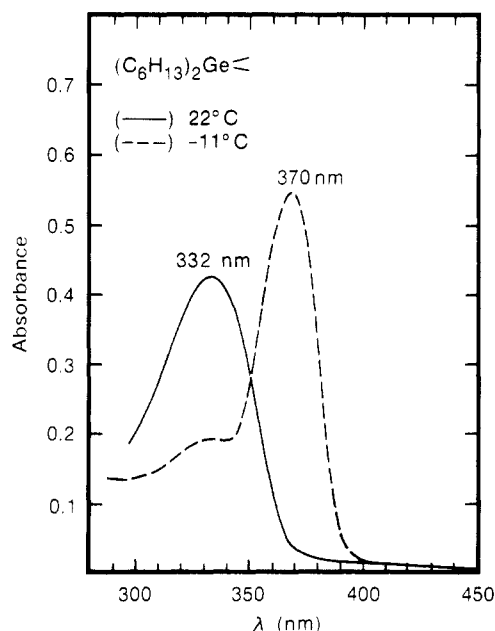


Figure 3. UV-absorption spectrum of poly(di-*n*-hexylgermane) as a function of temperature.

$\text{r}(\text{CH}_2)$ vibration in *n*-alkane urea clathrates, found at 1174 cm^{-1} , undergoes a pronounced intensity change at low temperatures and reflects a reduction in rotational mobility of the *n*-alkane chain in the urea channel. At room temperature this band broadens considerably and becomes quite weak. This may also explain the lack of a distinct band in the trimer, which can be assigned to the CH_2 rocking vibration since it may be too broad to observe at room temperature.

The remaining weak bands found in the $1000\text{--}1500\text{-cm}^{-1}$ region of the trimer are attributable to CC stretching vibrations of the butyl side chains. The presence of both 1063-cm^{-1} and 1083-cm^{-1} bands indicates that both trans and gauche CC bonds are present as would be expected in the liquid state. The assignments are summarized in Table I.

B. Poly(di-*n*-hexylgermane). Shown in Figure 3 are the UV-visible spectra of poly(di-*n*-hexylgermane) (PDHG) as a function of temperature. In contrast to the poly(di-*n*-alkylsilanes)^{1,2} where the observed thermochromic transition is at elevated temperatures, this transition in poly(di-*n*-hexylgermane) is below room temperature as seen by the predominance of the 370-nm peak at low temperatures in Figure 3. This is verified by the Raman spectra obtained at 488 nm and shown as a function of temperature in Figure 4. As can be seen, strong bands in

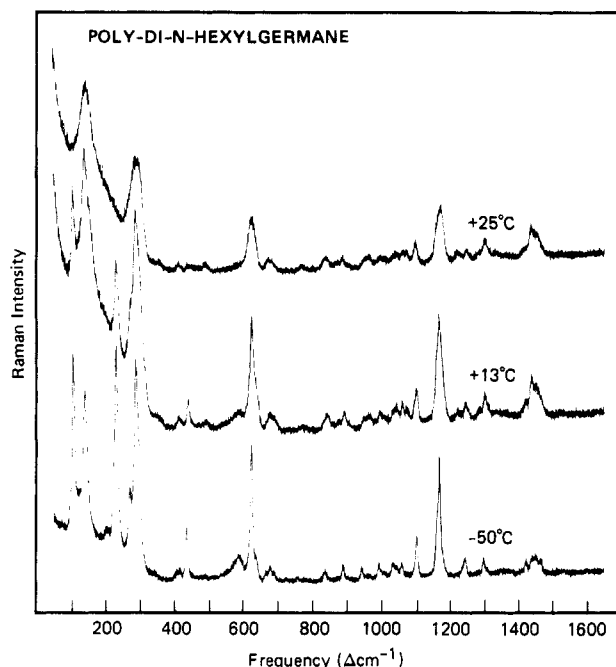


Figure 4. Raman spectra of poly(di-*n*-hexylgermane) obtained at 4880-Å excitation as a function of temperature. Thermochromic transition in PDHG occurs at 12°C .

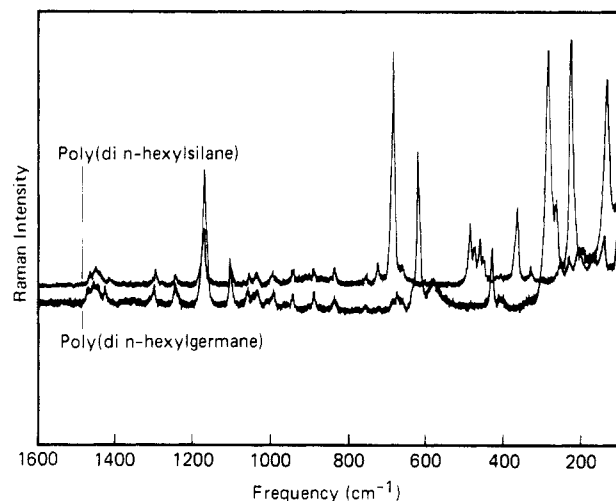


Figure 5. Comparison of Raman spectra of poly(di-*n*-hexylsilane) and poly(di-*n*-hexylgermane) in their ordered state (below their thermochromic transition temperature).

the low-frequency region characteristic of the vibration of Ge-Ge and Ge-C bonds sharpen below the transition temperature of $+12^\circ\text{C}$. In addition, there is a strong band at 1174 cm^{-1} that is much more intense than any of the other bands in this region and is attributable to the *n*-hexyl side chains. As shown in Figure 5 where the Raman spectrum of PDHG is compared with its silane analogue, a band at 1182 cm^{-1} with enhanced intensity was also observed in the latter, although the enhancement appeared to be somewhat less. In poly(di-*n*-hexylsilane) (PDHS), the 1182-cm^{-1} band was assigned¹⁰ to the vibration of the C-C bond attached to the Si backbone, based on isotopic-substitution studies. This band, as well as the Si-C stretch at 689 cm^{-1} , exhibited clear resonance enhancement behavior when their intensities were examined as a function of excitation frequency.⁶ The enhancement mechanism is unclear for the 1182-cm^{-1} band, but it is thought to be related to that responsible for the large intensity observed for the 689-cm^{-1} Si-C stretch, the bond adjacent to the C-C bond whose vibration is

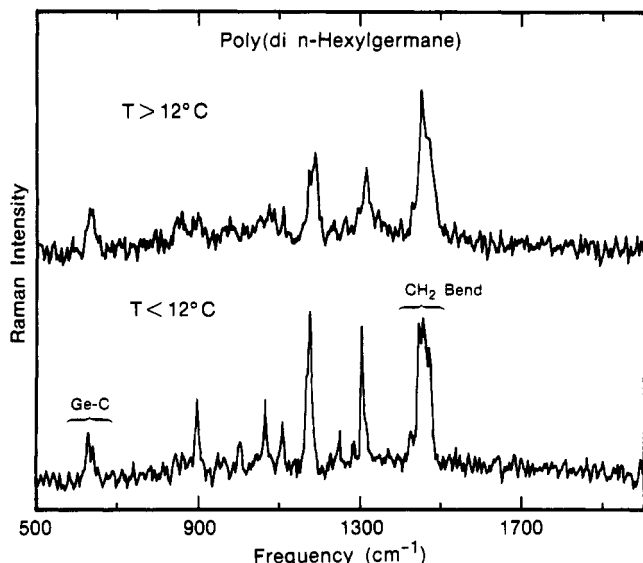


Figure 6. FT-Raman spectra of poly(di-*n*-hexylgermane) above and below its transition temperature.

found at 1182 cm^{-1} . Similarly, the enhancement of the intensity of the band at 1174 cm^{-1} in PDHG can be attributed to electronic interaction between the C-C vibration of the bond immediately adjacent to the Ge backbone with the Ge-C stretching vibration found at 633 cm^{-1} .

As observed in the 800–1500- cm^{-1} region of Figure 4, all other bands associated with vibrations of the *n*-hexyl side chains are considerably weaker than those associated with the backbone vibrations (Ge-Ge) even though the former represent a concentration of CH_2 groups 20 times larger. Certainly, as was shown previously for PDHS, this observation can be explained by the resonance or preresonance interaction between the visible laser excitation and the UV absorption of the Ge-Ge backbone chromophore at 370 nm. This resonance greatly enhances the Raman-scattering cross-section of those vibrations associated with the Ge backbone, and, hence, their intensity dominates the spectrum. Unfortunately, this complicates the interpretation of the weak CH_2 vibrations, which have poor signal-to-noise quality.

With the recent advent of FT-Raman spectroscopy,^{7,8} laser excitation in the infrared region has become possible, and this has allowed Raman spectra of PDHG to be obtained in the absence of significant resonance enhancement. The FT-Raman spectra of PDHG below and above its transition temperature (+12 °C) are shown in Figure 6. By comparison with similar data obtained by visible excitation (Figure 4), it becomes obvious that excitation at 1.064 μm yields a spectrum with little resonance enhancement. In fact, all bands observed in the 900–1500- cm^{-1} region are attributable to vibrations of the CH_2 groups, which appear with only low intensity in the conventional Raman spectra shown in Figures 4 and 5. As seen in Figure 6, the intensity of the Ge-C stretching vibration is considerably diminished, and its intensity more accurately reflects the concentration of these bonds in PDHG relative to the concentration of CH_2 groups (1:6).

An interesting observation regarding the conformation and intermolecular environment^{12,13} of the *n*-hexyl side chains can be made by considering the bands in the 1000–1200- and 1400–1500- cm^{-1} regions, respectively. The presence of strong bands at 1064 and 1106 cm^{-1} in the low-temperature spectrum indicates that the *n*-hexyl side chains adopt a planar zigzag conformation below the thermochromic transition similar to PDHS. Information about

the intermolecular packing of the side chains can be obtained upon considering the discrete splittings observed in the CH_2 bending region. The occurrence of intense bands at 1444, 1453, and 1469 cm^{-1} with a weaker, broad band around 1420 cm^{-1} may indicate^{12,13} a subcell structure containing more than one chain. Earlier Raman studies of odd *n*-alkanes¹³ have indicated that band-intensity patterns in this region could be correlated with X-ray diffraction measurements to verify the packing of chains into orthorhombic, monoclinic, and triclinic unit cells.

Two other pertinent observations regarding PDHG above the thermal transition can be made from the spectra ($T > 12^\circ\text{C}$) shown in Figure 6. As seen in the upper spectrum, the sharp, intense bands of the ordered state are replaced by broader, weaker bands. This is especially obvious in the 1000–1150- cm^{-1} region where the intensity of the 1060- cm^{-1} band is diminished relative to that at 1106 cm^{-1} and a new band at 1080 cm^{-1} is now observed between the much weaker 1064- and 1106- cm^{-1} bands. The presence of a 1080- cm^{-1} band is indicative of gauche bonds in the alkyl side chains and has been well documented in the case of long-chain fatty acids.¹⁴ This combined evidence suggests that the *n*-hexyl side chains become disordered above the thermochromic transition temperature for PDHG. A similar observation was made for poly(di-*n*-hexylsilane).¹⁰

A second observation concerning PDHG can be made upon comparison of the Ge-C stretching vibration at 633 cm^{-1} , which appears with equal intensity below and above the transition. Interestingly, although there is a significant change in UV absorption above 12 °C, which indicates that there must be some change in the overlap of electronic orbitals in the backbone, no apparent change in the bandwidth or intensity of the Ge-C stretch occurs. This is in marked contrast to that observed² in PDHS where the Si-C stretch shows a dramatic loss in intensity above the transition and broadens considerably so as to reflect a distribution of Si-C stretching frequencies. The behavior of the Ge-C band with temperature may reflect the slightly larger Ge-Ge bond distance (2.41 vs 2.35 Å for Si-Si), which relieves some of the steric interactions of adjacent *n*-hexyl side chains without a dramatic change in the local environment of the Ge-C bonds. This would also account for the difference in UV absorption found for both PDHS (316 nm) and PDHG (332 nm) above their transition temperatures. The longer wavelength absorption of PDHG reflects a less randomized organization of backbone (Ge-Ge) bonds than in PDHS, and, hence, the side chains may also be affected.

As discussed previously it becomes clear upon examination of the visible Raman spectra of Figure 5 and from the preceding discussions of the similarity between the FT-Raman spectra of PDHS and PDHG that the *n*-hexyl side chains (in each case) adopt a trans-planar conformation. Considering the similarity between silicon and germanium in conjunction with the common limiting absorption maximum below their respective transition temperatures, these observations suggest that their backbone conformations are also identical, i.e., that PDHG also adopts a planar, zigzag backbone at low temperatures. Consistent with this, recent wide-angle X-ray diffraction measurements¹⁵ on oriented PDHG have shown that the chain repeat distance is 4.0 Å, precisely that expected for a planar, zigzag backbone.

Conclusions

A series of germane oligomers and a polymer containing *n*-hexyl side chains has been investigated by Raman

spectroscopy in both the visible and near-infrared. In the latter, a thermochromic transition is observed at 12 °C with the UV absorption shifting from 372 to 332 nm. Spectroscopic results indicate that poly(di-*n*-hexylgermane) side chains adopt a trans-planar conformation similar to those of PDHS studied previously. In addition, FT-Raman studies of PDHG provided evidence that the interaction between the *n*-hexyl side chains was similar to that found in PDHS, suggesting that the germanium backbone, like its silicon analogue, can adopt a planar, zigzag conformation. Recent WAXD studies on oriented-PDHG samples have confirmed these findings.

The lowering of the transition temperature to +12 °C (compared to 42 °C for PDHS) is thought to reflect the larger Ge-Ge bond distances, which allow the onset of disorder to occur at lower temperatures. At the transition, the *n*-hexyl side chains disorder due to the introduction of gauche bonds. This change in interaction between the hexyl side chains allows the Ge backbone to adopt a disordered conformation, which somewhat interrupts the electronic overlap and results in a shift in absorption from 372 to 332 nm.

References and Notes

- (1) Miller, R. D.; Hofer, D.; Rabolt, J. F.; Fickes, G. N. *J. Am. Chem. Soc.* **1985**, *107*, 2172.
- (2) Rabolt, J. F.; Hofer, D.; Miller, R. D.; Fickes, G. N. *Macro-*

- molecules* **1986**, *19*, 611.
- (3) Schilling, F. C.; Bovey, F. A.; Lovinger, A. J.; Ziegler, J. M. *Bull. Am. Phys. Soc.* **1988**, *33*, 657.
- (4) Miller, R. D.; Farmer, B. L.; Fleming, W. W.; Sooriyakumaran, R.; Rabolt, J. F. *J. Am. Chem. Soc.* **1987**, *109*, 2509.
- (5) Farmer, B. L.; Miller, R. D.; Rabolt, J. F.; Fleming, W. W.; Fickes, G. N. *Bull. Am. Phys. Soc.* **1988**, *33*, 657.
- (6) Kuzmany, H.; Rabolt, J. F.; Farmer, B. L.; Miller, R. D. *J. Chem. Phys.* **1986**, *85*, 7413.
- (7) Hallmark, V. M.; Zimba, C. G.; Swalen, J. D.; Rabolt, J. F. *Spectroscopy* **1987**, *2*, 40.
- (8) Zimba, C. G.; Hallmark, V. M.; Swalen, J. D.; Rabolt, J. F. *Appl. Spectrosc.* **1987**, *41*, 721.
- (9) Miller, R. D.; Sooriyakumaran, R. *J. Polym. Sci., Polym. Chem. Ed.* **1987**, *25*, 111.
- (10) Hallmark, V. M.; Sooriyakumaran, R.; Miller, R. D.; Rabolt, J. F. *J. Chem. Phys.* **1989**, *90*, 2486.
- (11) Snyder, R. G.; Scherer, J. R.; Gaber, B. P. *Biochim. Biophys. Acta* **1980**, *601*, 47.
- (12) Snyder, R. G.; Hsu, S. L.; Krimm, S. *Spectrochim. Acta* **1978**, *34A*, 395.
- (13) Hendra, P. J.; Jobic, H. P.; Marsden, E. P.; Bloor, D. *Spectrochim. Acta* **1978**, *33A*, 445.
- (14) Lippert, J. L.; Peticolas, W. L. *Biochim. Biophys. Acta* **1972**, *282*, 8.
- (15) Farmer, B. L., private communication.

Registry No. PDHGe (homopolymer), 107310-68-9; PDHGe (SRU), 107258-58-2; 2,2-di-*n*-butyl-1,1,1,3,3,3-hexamethyltri-germane, 125330-39-4; chlorotrimethylgermane, 1529-47-1; dichlorodi-*n*-butylgermane, 4593-81-1; decamethyltetragermane, 14938-41-1; hexamethyldigermane, 993-52-2; chloropentamethyldigermane, 22640-93-3.

A Study of the Isothermal Crystallization Kinetics of Polyphosphazene Polymers. 2. Poly[bis(trifluoroethoxy)phosphazene]

Richard J. Ciora, Jr., and Joseph H. Magill*

Material Science and Engineering Department, University of Pittsburgh, Pittsburgh, Pennsylvania 15261. Received June 1, 1989;
Revised Manuscript Received November 7, 1989

ABSTRACT: The kinetics of isothermal crystallization of poly[bis(trifluoroethoxy)phosphazene] have been studied utilizing (i) a modified differential scanning calorimeter (DSC) technique and (ii) a depolarized light intensity (DLI) technique. The kinetics of transformation of the isotropic to 2-D pseudohexagonal mesophase (i.e. the sub T_m transformation) as well as the mesophase to 3-D orthorhombic phase (i.e. the sub $T(1)$ transformation) have been measured and analyzed by using Avrami analysis. Classical nucleation theory has been applied for estimating the interfacial surface free energy values for nucleation/crystallization behavior corresponding to the phase transformations in the sub $T(1)$ and sub T_m regions. In each instance the crystallization kinetics exhibit a very strong sensitivity to undercooling over a limited temperature span. Associated with each first-order transformation, the interfacial surface free energies are more than an order of magnitude lower than values obtained in the crystallization of regular homopolymers because of the more mutually compatible (mesophase) interfaces.

Introduction

The most recently developed inorganic based polymers that show considerable commercial potential are the polyphosphazene polymers. In general the polyphosphazene polymers consist of a chain backbone of alternating phosphorous and nitrogen atoms as illustrated in Figure 1. Common substituents on the phosphorous atom may include aryl, alkyl, aryloxy, alkoxy, amino, and halogens as well as several metal atoms and inorganic groups.

Different kinds of substituents on the phosphorous atom provide polymers that possess a wide variety of properties.^{1,2}

An interesting feature of these polymers is the fact that many of them exhibit mesophase behavior when heated from the three-dimensionally ordered crystalline state to the isotropic melt. The atomic/molecular structure of these phases for several polyphosphazenes is known.^{3,4} The effect of thermal cycling on the structure as well as the transition temperatures and enthalpies of these poly-